Hemming of Aluminum Alloy Sheets Using Electromagnetic Forming

Jianhui Shang, Larry Wilkerson, and Steve Hatkevich

Hemming is usually the last stage of production for automotive closures, and therefore has a critical effect on the quality of the final assemblies. The insufficient formability of aluminum alloys creates a considerable problem in the hemming process. To address this issue, electromagnetic forming was utilized to hem aluminum alloy sheets. Electromagnetic forming is a high strain rate forming process that is currently being investigated by both academia and industry. Past studies have shown that the formability of metals can be significantly improved during electromagnetic forming, which benefits the hemming of aluminum alloys. This article presents the experimental results of hemming Al 6061-T6 sheets using electromagnetic forming. The effects of the parameters of electromagnetic hemming on the hem quality are discussed. In addition, the numerical simulation results of electromagnetic hemming are presented to enhance the understanding of the process and to determine the efficacy on an industrial scale.

1. Introduction

Hemming is a process that bends the edge of a metal sheet to 180° or more. It serves several functions: to increase the part stiffness, to eliminate the acute edge, to improve the appearance of highly visible panel edges, and to join the inner and outer parts. Hemming is usually applied as the final stage of production for automotive closures. Therefore, hemming is critical to the actual part function, as well as the assembly quality.

Conventional hemming is a three-step process: bending, pre-hemming, and final hemming (Fig. 1). The first step (bending) is to bend the edge of a metal sheet to 90°. The second step (pre-hemming) is to bend the part 45° more, and the final step (hemming) is to fold the edge to 180° and create the hem union.

Hemming can be broadly categorized as two types: "2t" and "3t" (Fig. 2). A "2t" hem involves only a single sheet, and a "3t" hem involves two sheets (outer and inner). A fully flat hem requires materials with good formability, such as steel, because of the sharp hem radius that is required. For the materials with low formability, rope hems with larger hem radii are used to avoid strain localization and cracking produced by exceeding the forming limits.

Current initiatives in automotive industry are driving a need for stronger and lighter automotive panels. Light metals, such as aluminum alloys and magnesium, are being developed to reduce overall body weight and improve fuel economy. However, their lower formability tends to create considerable

problems. Aluminum alloys are difficult to hem because of their susceptibility to strain localization, which produces cracking on the flat hem edges (Ref 3). Thus, a rope hem instead of a flat hem is usually used for aluminum alloys.

A flat hem is more desirable than a rope hem because it has a better visual quality (Fig. 3). Carsley (Ref 4) identified the "apparent gap" as the distance between the tangent break lines of adjacent hemmed parts. The "apparent gap" is smaller between two flat hemming unions than it is between two rope hemming unions, which creates a better perception of overall quality (Ref 4).

There are several parameters to evaluate the hem quality of parts. One is the hem union radius, which is the distance between the edge of the hem union and the tangent break point (Fig. 3). The hem union radius is an important quality parameter for the "apparent gap." Another important hem quality parameter is "roll-in/roll-out", which refers to the position change of the bent edge after hemming (Ref 2). Large roll-in/roll-out could cause problems in the assembly stage. Therefore, these two parameters will serve as the basis to evaluate the hem quality in this study.

Several studies have been performed to improve the hem quality of aluminum alloys. Lin et al. (Ref 5) performed a computational design-of-experiment study for aluminum alloy 6111-T4 flat surface-straight edge "3t" hemming. They found that the pre-hemming die angle and the bending die radius significantly affect the roll-in/roll-out, and the pre-strain and the bending die radius greatly impact the maximum surface strain. Golovashchenko (Ref 6) presented a new method for the "3t" hemming of aluminum alloy 6111-T4. He applied a larger bending radius to redistribute the plastic strain. This new method allowed an additional 10% of pre-strain through the entire forming and assembly operations, and made it possible for the "3t" flat hemming of 6111-T4. Muderrisoglu et al. (Ref 7) carried out an experimental study on the "2t" hemming of aluminum alloy 1050. The results showed that cracks were observed on the outer surface over the bending area.

Jianhui Shang, Larry Wilkerson, and **Steve Hatkevich**, American Trim LLC, Lima, OH 45801. Contact e-mail: jshang@amtrim.com.
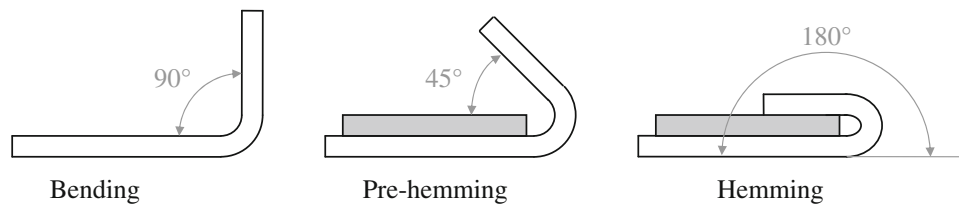
Fig. 1 Three stages of the conventional hemming process (Ref 1)

(a) "2t" flat hem   **(b)** "3t" flat hem

(c) "2t" rope hem   **(d)** "3t" rope hem
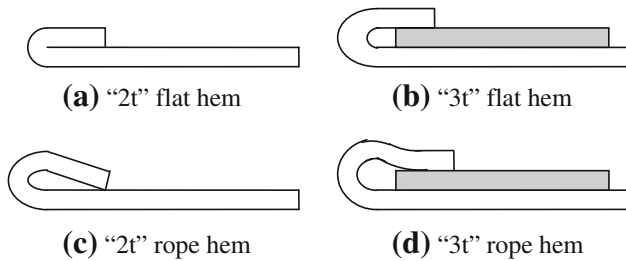
Fig. 2 Different types of hemming (Ref 2)

The aforementioned researchers focused on adjusting the parameters of conventional hemming, such as bending die radius and pre-hemming die angle.

Based on the observation of the improved formability in electromagnetic forming, Jimbert et al. (Ref 1) applied electromagnetic forming to the "3t" hemming of 6016-T4 aluminum alloys. The experimental results demonstrated that the electromagnetic (EM) hemming process produced the parts with a smaller hem union radius than those obtained by conventional hemming. He concluded the improvement was due to the wider and more uniform distribution of the deformation throughout the hemmed area produced by the high velocity forming. Jimbert also performed a numerical simulation on the electromagnetic hemming process, which confirmed the reduction of the maximum strain in electromagnetic hemming.

While Jimbert's study focused on the "3t" hemming, this article proposes to apply electromagnetic forming to the "2t" hemming of 6061-T6 aluminum alloys. Al 6061-T6 is not being used in automotive industry for outer skin panels. It was selected based on the material availability to this study. Besides, Al 6061-T6 exhibits low uniform elongation and high strength. If electromagnetic forming can produce reasonable hemming for Al 6061-T6, it would provide a new possible method to hem other aluminum alloys. In this method, electromagnetic forces are used to hem the pre-bent Al 6061-T6 sheet in one step, which eliminates the pre-hemming step. This article presents the experimental results to prove the viability of this method, while also presenting the numerical simulation results for better understanding of the electromagnetic hemming process.

2. Experimental Set-up of Electromagnetic Forming for Hemming

2.1 Background of Electromagnetic Forming

Electromagnetic forming is a technology whereby large electromagnetic forces are imparted to a conductive metallic workpiece. A typical electromagnetic forming system is composed of four different sections: the charging system, the capacitors, the coil and the workpiece. During electromagnetic forming, the capacitors are initially charged to the pre-set energy level by the charging system. Then the high current switch is closed to discharge the capacitors. During discharge, a large electric current moves through a conductive coil and produces a transient magnetic field around the coil. This magnetic field induces eddy currents in a nearby metal workpiece. The mutually repulsive electromagnetic pressure between the stationary coil and the metal workpiece can reach values exceeding 300 MPa; however, it typically only lasts for a short period on the order of 10 μs. This repulsive pressure will accelerate the metal workpiece to impact the die.

Electromagnetic forming usually is applied to accelerate metal workpieces at velocities up to a few hundred meters per second. Balanethiram and Daehn (Ref 8) and Seth et al. (Ref 9) have demonstrated that high velocity deformation can significantly increase the formability of metals compared to those obtained in conventional quasi-static forming. Daehn et al. (Ref 10) proposed that the extended formability is available over a broad range of deformation velocities, which is somewhat material dependent but generally lies over 50 m/s.

2.2 Experimental Set-up

Al 6061-T6 sheets with 0.8 mm thickness and a straight edge-flat surface hem configuration were used in this investigation. Sheet metal hemming involves various 3D geometric configurations. The straight edge-flat surface hem configuration is relatively simple, and therefore was studied here to prove the feasibility. The Al 6061-T6 sheets are manually bent to 90° (Fig. 4). The pre-bent Al 6061-T6 sheets are then hemmed using electromagnetic forming.

The EM coil is critical for electromagnetic forming, and should be designed to be close to the metal sheet where it needs
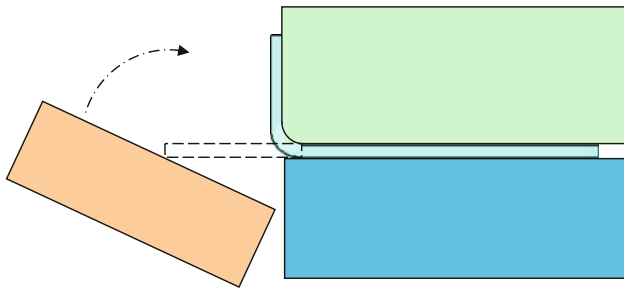

Fig. 3 Visual quality differences of hem unions—"flat-hemming" union used with steels (left) and "rope-hemming" union used with low formability alloys (right) (Ref 4)

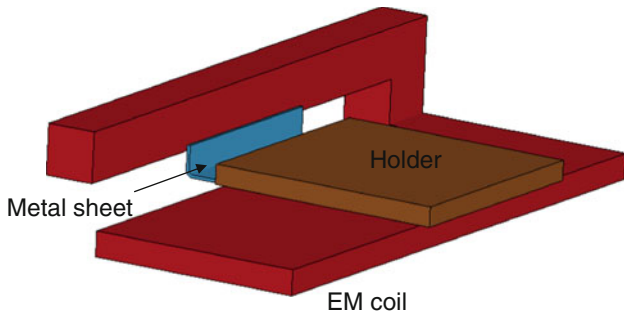**Fig. 4** Illustration of manual bending process in this study

Fig. 5 Straight-edge EM coil set-up for straight edge-flat surface hemming
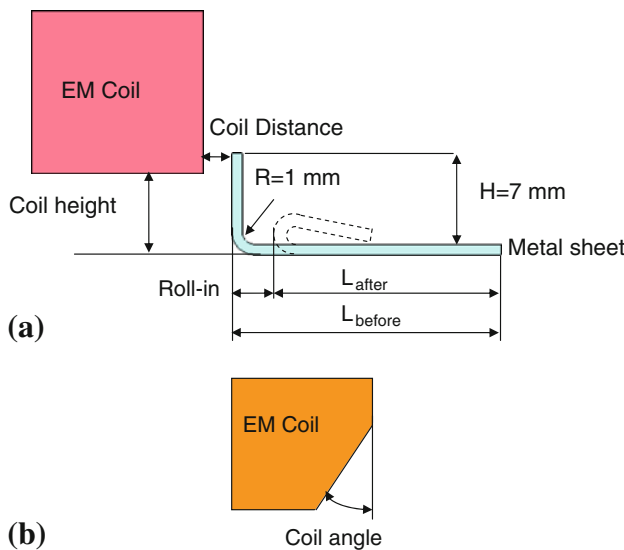

Fig. 6 Illustration of main experimental parameters: (a) coil height and coil distance; (b) coil angle

to be deformed. In this study, the flanged wall needs to be hemmed. Hence, the straight edge-flat surface coil was designed as shown (Fig. 5) to generate electromagnetic forces on the straight wall of the pre-bent Al 6061-T6 sheet. The holder was designed to clamp the flat section of the pre-bent Al 6061-T6 sheet to prevent the deformation.

All the Al 6061-T6 sheets were cut into 50 mm x 50 mm size, and then were manually bent to 90° with 1-mm bending radius and 7-mm bending height before EM hemming. Four parameters (Fig. 6) can influence EM hemming results:

Table 1 Design matrix of experiments and response

	Input varies				Response
Run	Energy input, kJ	Coil height, mm	Coil angle, °	Coil distance, mm	Roll-in, mm
1	1.8	9.5	30	0	1.96
2	7.2	4.8	30	0	0.19
3	7.2	4.8	30	2	2.55
4	7.2	4.8	0	0	7.29
5	7.2	9.5	0	2	1.09
6	7.2	4.8	0	2	0.19
7	1.8	9.5	30	2	1.74
8	1.8	4.8	30	0	2.23
9	1.8	4.8	0	0	0.64
10	1.8	9.5	0	2	0.15
11	7.2	9.5	0	0	1.29
12	7.2	9.5	30	0	1.12
13	1.8	4.8	30	2	0.28
14	7.2	9.5	30	2	0.19
15	1.8	9.5	0	0	1.10
16	1.8	4.8	0	2	0.73

(1) Energy input; (2) Coil height relative to the bent Al 6061-T6 sheet; (3) Coil distance between the EM coil and the bending edge; and (4) Coil angle. Traditionally, EM coil has a rectangular cross section that is parallel to the bending wall of metal sheet. In this study, one corner of the EM coil was machined to assess the relative influence of the coil angle on the EM hemming process.

An Elmag capacitor bank was used for each experiment. The maximum energy stored in this capacitor bank is 18 kJ with 360 μF capacitance at 10 kV charging voltage.

3. Design of Experiment

Table 1 displays the test matrix used for the experiment that was designed using a two-level full factorial design for the four factors. Factorial design is a statistics method to help determine the effects of factors. Factors are the parameters that can influence results. Two levels cover the possible range of each factor. After the 16 tests, the roll-in was determined as the difference between the L_{before} and L_{after} for each sample. L_{before} was measured before hemming as the distance between the flanged edge and the edge of the other side, and L_{after} was measured after hemming as the distance between the hemmed edge and the edge of the other side (Fig. 6). The software, Minitab 15, was applied to analyze the experimental data, and the Pareto Chart of the Standardized Effects (Fig. 7) clearly shows both energy input and coil height significantly affected the roll-in. Coil angle, coil distance, and the interactions between them are not statistically significant.

4. Further Study on Effect of Energy Input

4.1 Experimental Results

The previous 16 tests show that the energy input and the coil height affected the roll-in significantly. The effect of energy
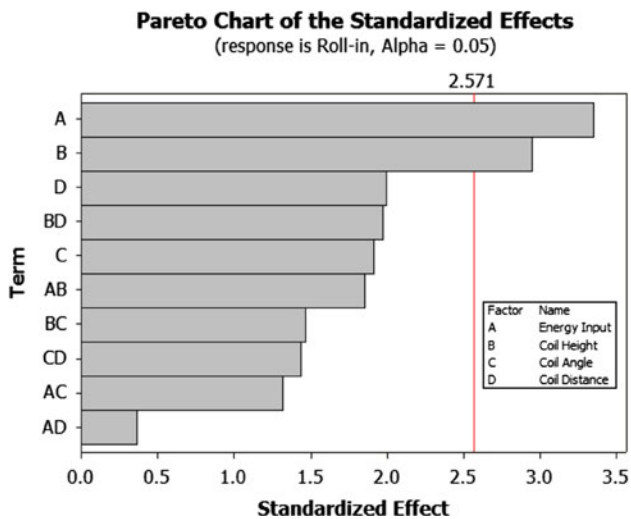
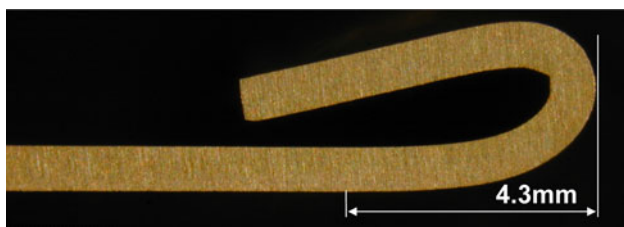**Fig. 7** Pareto chart of the standardized effects

Fig. 8 Cross-sectional view after EM hemming with 2.70 kJ energy input (roll-in: 0.84 mm; hem union radius: 4.3 mm)
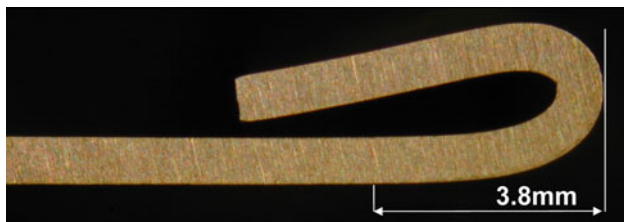

Fig. 9 Cross-sectional view after EM hemming with 3.24 kJ energy input (roll-in: 0.61 mm; hem union radius: 3.8 mm)

input will be studied in this section. Table 1 indicates that the coil height of 9.5 mm tended to produce smaller roll-in than the coil height of 4.8 mm. Therefore, the experimental conditions of 9.5-mm coil height, 0-mm coil distance, and 0° coil angle were chosen for the study of energy input. The four levels of energy input were applied to hem the Al 6061-T6 sheets that were pre-bent to 90°. Each sample was cut down the middle, polished, and then photographed in a cross-sectional view. As shown in Fig. 8, the tangent break point was determined as the tangent point of the straight bottom surface line of the flat section to the hem union curve. Then the distance between the tangent break point and the hem union edge was measured from the photo as the hem union radius. The roll-in was measured as the edge position change relative to the other side edge before and after hemming (Fig. 6). Following are the cross-sectional views of the samples for EM hemming with different energy inputs (Fig. 8-11).
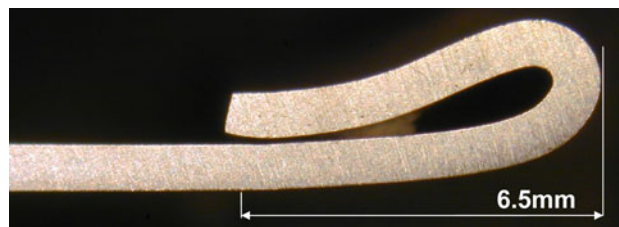

Fig. 10 Cross-sectional view after EM hemming with 3.60 kJ energy input (roll-in: 0.40 mm; hem union radius: 6.5 mm)

Fig. 11 Cross-sectional view after EM hemming with 7.20 kJ energy input (roll-in: 0.73 mm; hem union radius: 2.9 mm)
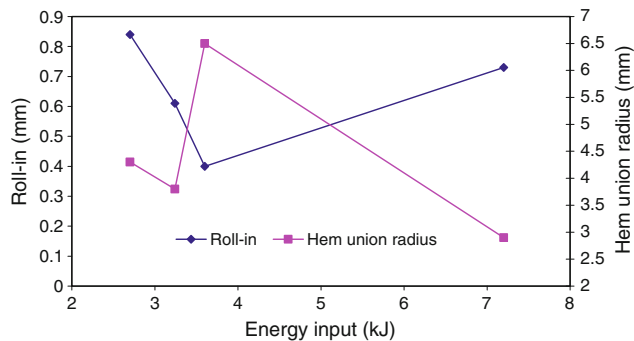

Fig. 12 Effects of energy input on roll-in and hem union radius (coil height: 9.5 mm)

Subsequently, the summary of the effects of energy input on the roll-in and the hem union radius is shown (Fig. 12). It shows that the roll-in decreased with the increase of energy input. However, excessive energy input (7.20 kJ) resulted in an increased roll-in. The hem union radius decreased with the increase of energy input from 2.70 kJ to 3.24 kJ. But at an energy input of 3.60 kJ, the hem union was bent upwards significantly and had a larger hem union radius (6.5 mm). When the energy input was increased to 7.2 kJ, the hem union radius decreased to 2.9 mm. It should be noted that at an energy input of 7.20 kJ, the bending edge impacted onto the flat section and the flat section was no longer flat. This is an unacceptable hem condition.

Based on the results of this analysis, an energy input of 3.24 kJ produced a smaller hem union radius with a smaller roll-in, and thereby produced the best hem quality among the four test conditions.

4.2 Comparison Between EM and Conventional Hemming

An Al 6061-T6 sheet was hemmed via conventional hemming to compare to EM hemming. As in the case of the EM tests, the part was manually bent to 90° (Fig. 4), then

pre-hemmed to 135°, and then hemmed to 180°. The resulting part was cut down the middle, polished, and photographed in a cross-sectional view (Fig. 13). The roll-in and the hem union radius were determined with the same methods used for the EM hemming.

Comparing Fig. 13 to Fig. 9, the EM hemmed part at 3.24 kJ had a smaller roll-in than the part produced with conventional hemming, which indicates that the EM hemmed part had a better dimensional accuracy. Moreover, the EM hemmed part had a smaller hem union radius than the part produced with conventional hemming. The smaller "apparent gap" produced by the EM hemming process suggests that EM hemmed parts may have a better overall perceived quality than a conventionally hemmed part.

It should be noted that the conventional hemming part in Fig. 13 was manually bent and hemmed, and does not represent the current state-of-the-art for aluminum alloy hems. However, the results of this study do demonstrate that the EM hemming process produces a competitive hem quality for representative aluminum alloy hems. They also indicate that this process may be feasible on an industrial scale. Clearly, optimization is necessary to refine the EM hemming technique and to improve the overall hem quality.
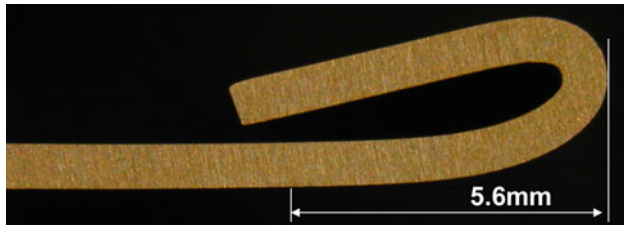
Fig. 13 Cross-sectional view after conventional hemming (roll-in: 1.04 mm; hem union radius: 5.6 mm)

5. Numerical Simulation

5.1 Simulation Model Development

Electromagnetic forming is a complex forming process, involving mechanical, thermal and electromagnetic phenomena. It is difficult to analyze and predict this process. To develop a better understanding of the EM hemming process, a numerical simulation was performed using the LS-DYNA electromagnetism module available in the "beta" 980 version. In this module, the finite element method (FEM) is coupled with the boundary element method (BEM) to determine the magnetic fields, electric fields and induced currents by solving Maxwell equations in an eddy-current approximation. FEM is applied to solve Maxwell equations for the solid conductors and BEM is used for the surrounding air. The detailed introduction of this module can be found in Ref 11.

The 3D simulation model of the EM hemming process was built for LS-DYNA (Fig. 14). There were three parts: the Cu straight single-turn coil, the pre-bent Al 6061-T6 sheet, and the G10 Garolite holder. The Cu coil and the Al 6061-T6 sheet were modeled using eight-node hexagonal solid elements, which are required for the solid conductors in the electromagnetism module. The flat section of the Al 6061-T6 sheet under the G10 holder had coarser meshes than the bent section because the flat section did not undergo plastic deformation during EM hemming, and the coarser meshes would save computing time. The G10 holder was modeled as rigid body with shell elements, since the G10 holder did not undergo plastic deformation during EM hemming and is electrically non-conductive.

Since this EM hemming process involves high strain rate and large deformation, Cu and Al 6061-T6 were modeled using
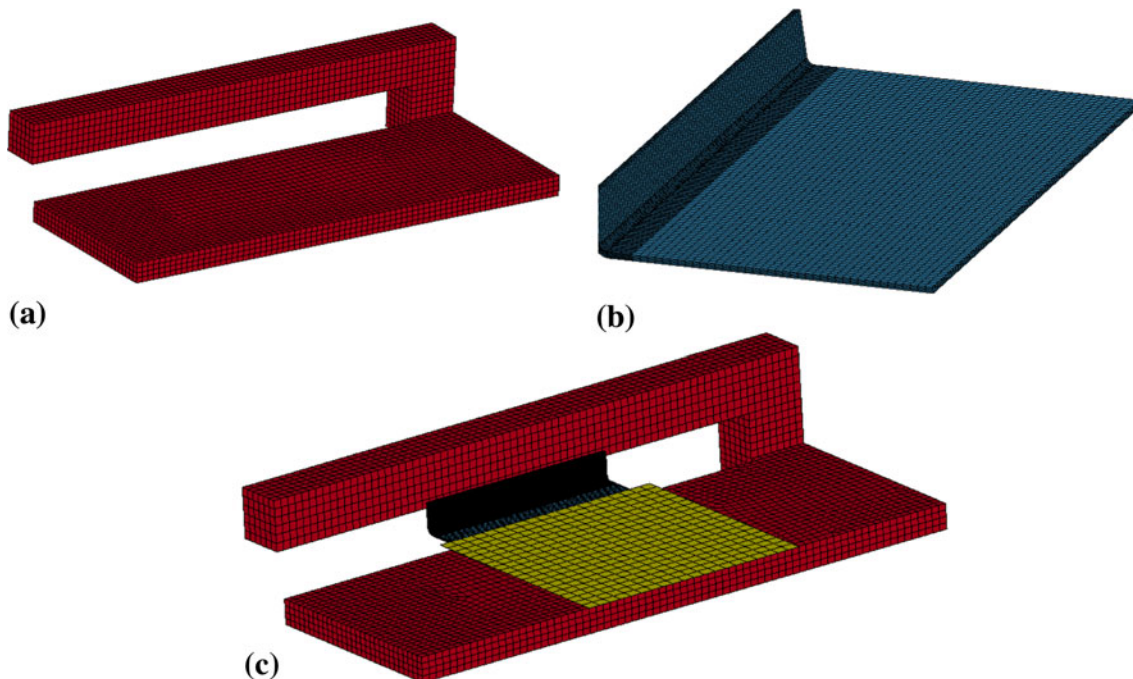
Fig. 14 Meshed models for the simulation (a) Cu coil; (b) Al 6061-T6 sheet; (c) assembly of Cu coil, Al 6061-T6 sheet and G10 holder

the Johnson-Cook strength model, which has the following form (Ref 12):

$$\sigma = (A + B\varepsilon^n)(1 + C \ln \dot{\varepsilon})\left[1 - \left(\frac{T - T_{room}}{T_m - T_{room}}\right)^m\right]$$

Table 2 lists the Johnson-Cook strength model parameters for Al 6061-T6 and Cu used in this simulation. Table 3 lists the material properties of Al 6061-T6 and Cu. The measured current trace in Fig. 15 was set as the input for the simulation in the 2.7 kJ energy input case.

Table 2 Johnson-Cook strength model parameters

Material	A, MPa	B, MPa	C	n	m	T_m, K
Al 6061-T6 (Ref 13)	324	114	0.002	0.42	1.34	925
Cu (Ref 14)	90	292	0.025	0.31	1.09	1331

Table 3 Material properties of Al 6061-T6 and Cu

Property	Al 6061-T6 (Ref 15)	Cu (Ref 14)
Electrical conductivity, $10^6/\Omega$ mm	0.0251	0.0588 (Ref 15)
Mass density, g/mm^3	0.0027	0.00896
Young's modulus, GPa	68.9	124
Poisson's ratio	0.33	0.34
Specific heat capacity, J/g °C	0.896	0.383
Thermal conductivity, W/m K	167	385 (Ref 15)
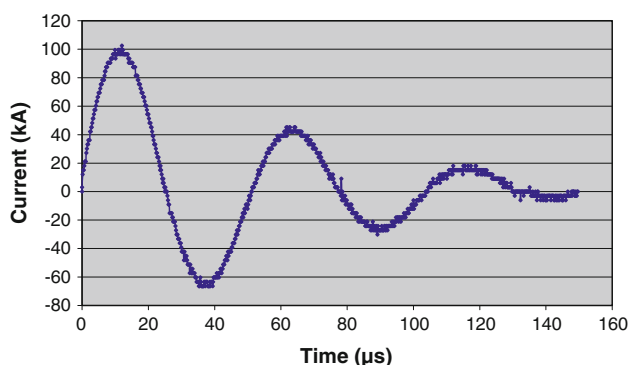
Fig. 15 Measured current trace in the coil in 2.7 kJ case
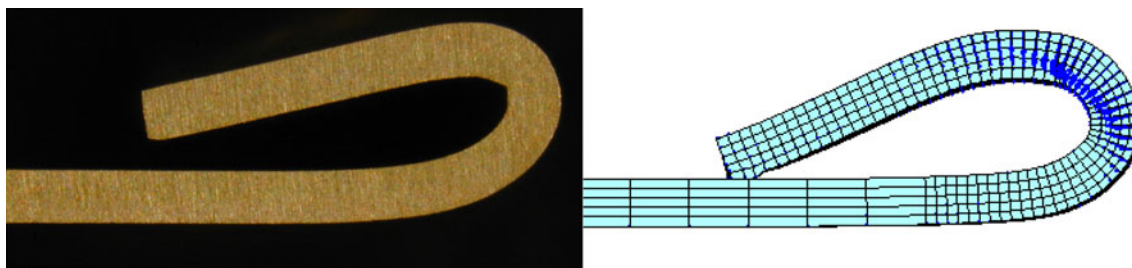
5.2 Comparison Between Experimental and Numerical Results

Figure 16 presents the comparison between the experimental and numerical simulation results for the 2.7 kJ energy input case. It shows that the numerical simulation result overestimated the EM hemming deformation. There was approximately a 0.3-mm gap between the hemming edge and the top surface of the flat section. However, the hemming edge impacted onto the top surface of the flat section in the numerical simulation. One possible reason for the overestimation is that the part was physically bent to 90° prior to the electromagnetic hemming. The pre-bending was not considered in the numerical simulation. Therefore, the strain-hardening prior to the electromagnetic hemming was not included in the numerical simulation, which might affect the simulation result.

5.3 Lorenz Force Distribution

During electromagnetic forming, workpiece is accelerated and deformed through Lorenz forces between coil and workpiece that is difficult to predict due to the complexity of electromagnetic forming. Lorenz forces vary over time and location. But accurate prediction of Lorenz forces is critical to achieve the desired deformation. The numerical simulation in this study provided insight about the variation of Lorenz forces during EM hemming, which is helpful to design EM hemming coil and process. Figure 17 presents the Lorenz force distribution in the middle section at the different time steps. At the early stage, the repulsive Lorenz forces concentrated on the upper area of the bent wall and then moved the upper area forward first. With the movement of the upper area, the attractive Lorenz forces occured to act on the upper area and the repulsive Lorenz forces acted on the rest of the bent wall at the 20-μs time step. The bent wall continued to move forward as a result of inertia. The repulsive Lorenz forces concentrated again on the small upper area of the bent wall at the 30-μs time step. With the increase of the gap between the bent wall and the coil, the coupling between them became weaker and weaker. In turn, the Lorenz forces on the bent wall became smaller and smaller. The bent wall moved down due to inertia and impacted on the flat surface at the 63-μs time step.

Figure 17 clearly shows that the Lorenz force distribution varied at the different areas along the bent wall and also changed with the time step. In addition, the Lorenz forces were large at the early stage, i.e., the first half cycle of the discharge. After that, the Lorenz forces became smaller and smaller.
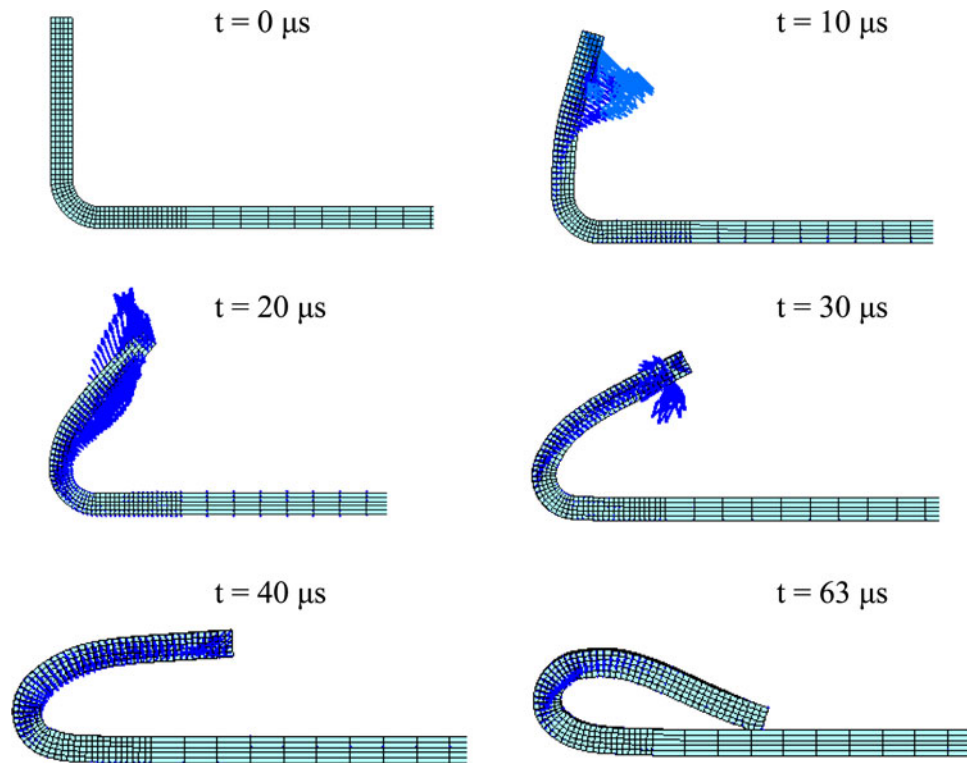

Fig. 16 Comparison between experimental and numerical results for the case of 2.7 kJ and 9.5-mm coil height (left: experimental result; right: numerical result)

Fig. 17 Lorenz force distribution in the middle section at different time steps (energy input: 2.7 kJ; coil height: 9.5 mm)

6. Summary

This study presents an innovative approach to hem aluminum alloys using electromagnetic forming. Using the hem union radius and the roll-in as metrics, the experimental results demonstrated that the EM hemming is capable of producing hems in Al 6061-T6 sheet with similar or better levels of quality as conventional hemming. Moreover, EM hemming eliminated the pre-hemming stage and could hem the pre-bent parts from 90° to 180° in one step. The study also indicated that both energy input and coil height significantly affected the quality of the final hem. The numerical simulation results showed that the Lorenz force distribution varied at different areas along the bent wall and also changed with the time step.

This study proves the feasibility of electromagnetic forming for "2t" hemming of aluminum alloys. More optimization is needed in the future to refine the EM hemming technique to improve hem quality. A numerical simulation with consideration of strain hardening prior to electromagnetic hemming will be beneficial for a better understanding of the process.

References

1. P. Jimbert, I. Eguia, I. Perez, M.A. Gutierrez, and I. Hurtado (2010) Analysis and Comparative Study of Factors Affecting Quality in the Hemming of 6016-T4AA Performed by Means of Electromagnetic Forming and Process Characterization, *J. Mater. Process. Technol.*, 2011, **211**(5), p 916–924

2. G. Zhang, H. Hao, X. Wu, S.J. Hu, K. Harper, and W. Faitel, An Experimental Investigation of Curved Surface-Straight Edge Hemming, *J. Manuf. Processes*, 2000, **2**(4), p 241–246

3. G. Lin, "Quality and Formability of Automotive Aluminum Alloys," Dissertation, The University of Michigan, Ann Arbor, MI, 2006

4. J.E. Carsley, Microstructural Evolution During Bending: Conventional vs. Roller Hemming, *Trends in Materials and Manufacturing Technologies for Transportation Industries*, T.R. Bieler, J.E. Carsley, H.L. Fraser, J.W. Sears, and J.E. Smugeresky, Ed., TMS, 2005, p 169–174

5. G. Lin, K. Iyer, S.J. Hu, W. Cai, and S.P. Marin, A Computational Design-of-experiments Study of Hemming Process for Automotive Aluminum Alloys, *J. Eng. Manuf.*, 2005, **219**(10), p 711–722

6. S. Golovashchenko, Sharp Flanging and Flat Hemming of Aluminum Exterior Body Panels, *J. Mater. Eng. Perform.*, 2005, **14**, p 508–515

7. A. Muderrisoglu, M. Murata, M.A. Ahmetoglu, G. Kinzel, and T. Altan, Bending Flanging, and Hemming of Aluminum Sheet—An Experimental Study, *J. Mater. Process. Technol.*, 1996, **59**(1–2), p 10–17

8. V.S. Balanethiram and G.S. Daehn, Hyperplasticity-Increased Forming Limits at High Workpiece Velocities, *Scripta Metall.*, 1994, **31**, p 515–520

9. M. Seth, V.J. Vohnout, and G.S. Daehn, Formability of Steel Sheet in High Velocity Impact, *J. Mater. Process. Technol.*, 2005, **168**(3), p 390–400

10. G.S. Daehn, V.J. Vohnout, and L. DuBois, Improved Formability with Electromagnetic Forming: Fundamentals and a Practical Example, *Sheet Metal Forming Technology*, M.Y. Demeri, Ed., The Minerals, Metals & Materials Society, 1999, p 105–116

11. P. L'Eplattenier, G. Cook, and C. Ashcraft, Introduction of an Electromagnetism Module in LS-DYNA for Coupled Mechanical Thermal Electromagnetic Simulations, *Proceedings of 3rd International Conference on High Speed Forming*, M. Kleiner and

A.E. Tekkaya, Ed., March 11–12, 2008 (Dortmund), Technical University Dortmund, p 85–96

12. G.R. Johnson and W.H. Cook, A Constitutive Model and Data for Metals Subjected to Large Strains, High Strain Rates and High Temperatures, *Proceedings of 7th International Symposium on ballistics*, April 1983, The Hague, The Netherlands, p 541–547

13. B.M. Corbett, Numerical Simulations of Target Hole Diameters for Hypervelocity Impacts into Elevated and Room Temperature Bumpers, *Int. J. Impact Eng.*, 2006, **33**, p 431–440

14. G.R. Johnson and W.H. Cook, Fracture Characteristics of Three Metals Subjected to Various Strains, Strain Rates, Temperatures and Pressures, *Eng. Fract. Mech.*, 1985, **21**, p 31–48

15. http://www.matweb.com, Accessed, October 8, 2010